Unusual mixed silica–carbonate deposits from magmatic-hydrothermal hot springs, Savo, Solomon Islands

D.J.Smith[1]*, G.R.T. Jenkin[1], M.G.Petterson[1], J. Naden[2], S. Fielder[1], T. Toba[3], S.R.N. Chenery[2]

1. University of Leicester, Leicester, LE1 7RH, UK

2. British Geological Survey, Keyworth, Nottingham, NG12 5GG, UK

3. Geology Division, Ministry for Energy, Mines, and Rural Electrification, Honiara, Solomon Islands

(*corresponding author djs40@le.ac.uk)

Abstract

The volcanic island of Savo, Solomon Islands, hosts an active hydrothermal system discharging unusual alkaline (pH 7–8) sulphate-rich, chloride-poor fluid, with variable admixtures of Ca–Mg–HCO_3^- rich fluid. Hot springs and their outflow streams precipitate a variety of deposits, including travertine, silica sinter and unusual mixed silica–carbonate rocks. Travertine fabrics are dominated by ray-crystal calcite, associated with rapid abiotic precipitation from a supersaturated solution. Sinter is produced by evaporation of thermal waters, and downstream samples contain preserved traces of micro-organisms, which potentially acted as templates for precipitation. Trace element chemistry of sinters and travertines includes anomalously high levels of Te, indicating a magmatic origin for a component fluid in the hydrothermal system. Springs are close to or at saturation with both calcite and amorphous silica. Increased contributions from the Ca–Mg–HCO_3^- end-member favours calcite formation; this fluid is of low temperature origin, and as such is favoured by high rainfall. Mixed samples show cyclical changes between silica and carbonate precipitation, potentially as a result of seasonal variation in rainfall.

Supplementary material: Spreadsheet of water and deposit chemical analyses is available at www.geolsoc.org.uk/SUP00000

[INTRODUCTION]

Travertine ($CaCO_3$) and siliceous sinter (using the terminology of Renaut & Jones, 2003) are common features around hot springs and the streams they feed. However, mixed silica–carbonate deposits are rare, with only a few recognised worldwide, most notably at Ohaaki, Ngatamariki, and Waikite, New Zealand (Jones *et al.* 1996; Campbell *et al.* 2002; Jones & Renaut 2003a). On Savo (Solomon Islands), a volcano with an active magmatic–hydrothermal system (Smith et al. 2010), highly unusual mixed deposits, accompanied by separate deposits of sinter and travertine are commonly found at springs and thermal streams.

Sinter is most commonly associated with discharge of near-neutral, chloride-rich thermal waters (Hedenquist *et al.* 2000) that have reacted with host rocks at temperatures in excess of 175°C (Fournier & Rowe 1966; Uysal *et al.* 2011), or more rarely with acid sulphate waters (Rodgers *et al.* 2004) and acid sulphate-chloride waters (Schinteie *et al.* 2007). However, the fluids discharged at Savo are alkaline sulphate fluids with very low chloride (Smith *et al.* 2010). Thus, the alkaline sulphate springs on Savo represent an environment of sinter formation not previously described. It is important to understand the range of environments and fluids that form sinters – and the nature of the sinters that different environments produce – if deposits in the geological record are to be interpreted properly. Furthermore, as the study of surface hydrothermal deposits provides information on the origin of life and mineral–microbe interactions (e.g. Farmer 2000), it is important to understand the range of chemical and physical environments in which they form.

In some cases sinter can be the surface manifestation of a mineralised system (Vikre 2007) and therefore an indicator of gold-bearing palaeo-hydrothermal and hydrothermal systems (Hedenquist *et al.* 2000; Uysal *et al.* 2011). As Savo occurs in a region prized for epithermal gold deposits (e.g. Ladolam, Lihir, Papua New Guinea; Carman 2003) might hydrothermal deposits, like those on Savo, be a useful indicator of potential mineralisation?

This paper describes the morphology and mineralogy of travertine, sinter and mixed silica–carbonate deposits on Savo, their chemistry and the waters from which they precipitate. The aims of the study are: 1) to identify the mechanisms which precipitate travertine, sinter and mixed deposits; 2) to determine the processes behind changes between carbonate-dominant, silica-dominant and mixed deposit precipitation; 3) to determine the significance of trace element concentrations in the precipitates.

Background

Savo is a recently active volcano in the central Solomon Islands (Fig. 1), dominated by sodic trachyte and mugearite rocks (Smith *et al.* 2009). Eruptive activity (last eruption 19th century) has been dominated by dome formation and subsequent collapse to pyroclastic debris currents (Petterson *et al.* 2003). At present, an active hydrothermal system manifests at the surface in a series of hot springs and fumaroles. Smith *et al.* (2010) discussed the chemistry of the various springs in detail. In brief, high temperature (>80°C) springs are divided into two main classes – (1) acid sulphate hot springs (pH 2–7) of steam heated origin, and (2) more voluminous alkaline sulphate springs (pH 7–8), that are dilute, chloride-poor (< 50 mg/l), and sulphate- (> 600 mg/l) and silica-rich (> 250 mg/l). Table 1 summarises the chemistry of alkaline sulphate type springs. There are a number of lower temperature (25–60°C) bicarbonate-sulphate springs around the island that discharge fluids with (relative to the alkaline sulphate springs) lower silica and sulphate concentrations, and higher bicarbonate, Mg and Ca contents (Table 1).

Smith *et al.* (2010) interpreted the hot springs at Savo as the output of a magmatic-hydrothermal system that has been subject to considerable dilution by meteoric-derived waters. Weather stations on Guadalcanal record monthly average rainfalls of ~25 cm in the November–April wet season and ~10 cm in the April–November dry season (Solomon Islands Meteorological Service, www.met.gov.sb).The hot spring compositions indicate that the subsurface of the volcano can be considered an open system, with considerable mixing between end-member fluids leading to intermediate water types. In particular, alkaline sulphate hot springs of the Crater Wall/ Poghorovorughala area (Table 1) show enhanced bicarbonate, Mg and Ca contents relative to the Eastern/Rembokola springs, indicating mixing of a lower temperature Ca, Mg-rich water into a hotter, hydrothermal silica-rich water. Water-rock equilibration temperature for the high temperature, silica-contributing end-member was estimated to be 260°C (Smith *et al.* 2010).

Distribution, morphology and mineralogy

Rembokola Valley

The Rembokola stream, on the east side of the island (Fig. 1), is fed by hot springs on the upper flanks of the volcano. These springs discharge small volumes (<0.5 litres per second) of fluid, and have produced terraced sinter deposits (Fig. 2A). Individual benches are no more than a few square centimetres in area, thus in the terminology of Fouke *et al.* (2000) are

considered micro-terracettes. The sinter is highly porous and friable opal-A (X-ray amorphous silica, using a Philips PW 1716 X-ray diffractometer; Fig. 2B) with small amounts of anhydrite. Small silica-encrusted filaments (<5 μm diameter) are visible in places, particularly within pore spaces (Fig. 2C).

Downstream, in an area of vigorous hot springs discharging directly into the stream, sinter grows above the water surface on detritus, usually developing into small (1–2 cm) pointed columns (Fig. 3A). SEM analysis of the spicular sinter shows that it is opal-A, often with anhydrite crystals on the top surface (Fig. 3B). This spiculose sinter is similar in appearance to that from Ngatamariki stream, New Zealand, as described by Campbell *et al.* (2002).

Downstream of the springs sinter coats and cements sediment and leaf litter in the stream channel, and forms crusts in the stream channel and banks where accumulations are thicker (Fig. 4A). It is typically finely laminated (layers <1 mm; Fig. 4B). Some of the layers are non-porous opal-A (Fig. 4C), others a mixture of non-porous opal-A and hollow, opal-A encrusted filaments up to 5 μm in diameter and 100 μm in length (Fig. 4D, E), aligned orthogonally to the layers. This laminated sinter facies occurs from within a few metres of the springs, to the mouth of the stream.

In some locations along the Rembokola stream, mixed silica–carbonate terraces occur above the current water level (upper surface approximately 30 cm above water level at time of observation in dry season, April–November; Fig. 5A). It is unclear from the field relations as to whether the mixed deposits represent high-water level deposits (i.e. wet season, Nov–April) or older deposits on the margins of the stream channel that have been eroded away from the active channel. The exposed surfaces of the mixed show signs of weathering, erosion and lichen colonisation, suggesting that they represent the remnants of older deposits, rather than recent or latest wet season deposits.

The mixed deposits consist of alternating layers of opal-A and calcite (XRD). Individual layers are up to 10 mm thick, and unconformities are common (Fig. 5B, D). Carbonate layers are formed from ray-crystals of calcite (Folk *et al.* 1985; Chafetz & Guidry 1999) organised into near-vertical fans (Fig. 5C). Silica layers are mainly non-porous, but in cavities where a three dimensional view is possible, small filaments are visible (Fig. 5E). Porosity and internal structure appears to have been infilled/ overprinted by continued silica precipitation (Jones & Renaut 2003a), again suggesting that the mixed deposits are older than the layered sinters (which still preserve abundant filament structures and porosity).

Poghorovorughala Valley

Deposits form around alkaline sulphate hot springs and in the base of the stream. Deposits are carbonate-dominated (aragonite and calcite, with possible minor dolomite indicated by XRD) with opal-A. Distinct depositional facies can be observed (Fig. 6A):

1) Lobate deposits form adjacent to alkaline sulphate springs, in areas frequently splashed and bathed by thermal waters. They typically have smooth, rounded upper surfaces of carbonate (microcrystalline aragonite or calcite) with opal-A and minor anhydrite (Fig. 6A–D). Individual lobes are finely laminated in cross section (Fig. 6B). The cores/ bases of the concentric layers often contain portions of the substrate (typically kaolinite, formed by steam heated alteration of volcaniclastic host sediments; Fig. 6B). Trigonal prisms of calcite are visible in SEM images, typically in sheltered areas between lobes (Fig. 6E, G–H). Pyrite and some manganese oxide precipitate on the underside of the lobes (i.e. slightly submerged or at the contact with the hot spring water; Fig. 6F).

2) Spicular deposits form slightly further from the springs, typically in areas splashed and bathed infrequently. The physical appearance is identical to the spiculose sinter near the Rembokola springs (Fig. 3), although contains much more carbonate. Spicular growths were observed developing on a lobate travertine substrate (Fig. 6A).

3) Interlayered silica–carbonate deposits occur in the discharge channels of springs and in the stream. The ~3 m high Mound Spring (Fig. 7A) is constructed of layered precipitates (based on surface exposure) with micro-terracetted surface texture (Fig. 7B). The layers are 5–50 mm thick, and generally pale in colour, although some dark layers do occur (Fig. 7C). Dark layers tend to be dominated by opal-A (Fig. 7D); whereas the pale layers are composed of ~1 mm long calcite ray-crystals organised into fans that diverge upwards (Fig. 7F; mineralogy confirmed with XRD). Minor anhydrite is present, mostly within the carbonate dominated layers (Fig. 7G).

Tanginakulu Valley

Travertine occurs in the stream channel along the entire length of the Tanginakulu stream. In relatively flat areas, travertine coats and cements stream detritus; whereas greater thicknesses of layered travertine develop at rapids and waterfalls (Fig. 8A). Layers are finer than those observed in the Poghorovorughala layered travertine (generally <5 mm thick), but the calcite has a similar morphology of elongate calcite ray-crystals in upwards-diverging fans (Fig. 8B–C).

Analytical methods

Bulk samples were powdered in a steel jaw crusher and agate planetary mill. Other samples were obtained by drilling out individual layers. At the British Geological Survey (BGS), Keyworth, for each sample 0.1 g powder was dissolved in a mixture of 2 ml H_2O and 2 ml aqua regia. HF acid was added to samples to dissolve any silica (1 ml for sinters, and mixed samples; 0.2 ml for travertines). Resulting mixtures were heated to 40°C for one hour to encourage complete dissolution, then left to dry overnight at 120°C. Dried samples were redissolved in a mixture of 1.2 ml H_2O, 0.4 ml HCl and 0.9 ml HNO_3, and warmed to 40°C for 30 minutes. Following complete dissolution, 10 ml H_2O and 2.5 ml H_2O_2 was added, followed by a further dilution with 10 ml H_2O. All H_2O was 18.2 MΩ quality. Samples were analysed at BGS using an Agilent 7500 series ICP-MS in helium gas collision cell mode to minimise spectral interferences. The instrument was calibrated with a series of ISO17025 traceable multi-element solutions (SPEX CertiPrep™). A series of quality control standards independent of the calibration solutions were analysed throughout each run. Precision and bias of these chemical solutions was better than +/-10% and typically better than +/-5%. Four analyses of BCR-2 reference material (values taken from GeoReM – http://georem.mpch-mainz.gwdg.de) typically yielded precision and bias better than +/- 15% with notable exceptions being Ni bias -36% and Cu bias -18%.

A subset of bulk powders was analysed at Acme Analytical Laboratories, Canada. Samples were crushed and powdered as above, and analysed by ICP-MS following aqua regia digestion. Precision and accuracy were estimated by duplicate analysis of laboratory standard DS7; precision (2σ) was <5% for all species except Zn, Se, Ag (<15%); Cu (43%) and Au (63%). The low reproducibility of Cu and Au indicates a nugget effect with standard DS7. Similar values were obtained for repeat analysis (n = 4) of a Savo carbonate. The accuracy (mean measured DS7 vs. accepted value) was better than +5% for Mn, V, Zn; −5% for Ag, Pb, Se; 10% for As, Au, Ba, Cd; +15% for Sr, Cu; −12% for Sb; and +19% for Te. The full dataset is included in the supplementary data.

Water samples were collected and analysed as per Smith *et al.* (2010).

Results

Streams

The Rembokola stream is fed by alkaline sulphate hot springs in the Toakomata area (the area immediately around sample locations a–c, Fig. 1), and has a similar chemistry, with high Na, Ca, Si, K, and SO_4^{2-}, and low Cl^- (Table 2). Arsenic occurs in concentrations of 60–70 μg/l; for comparison, typical seawater concentrations are only 1 μg/l (Cabon & Cabon 2000). The chemistry shows no abrupt downstream changes, reflecting the fact that there are no tributaries. There are, however, gradual changes to the stream chemistry including a downstream decrease in temperature, DIC, Mn, and Si; and an increase in Cl^-, and pH (Table 2, Fig. 9).

The Tanginakulu stream is fed by low discharge warm springs of bicarbonate-sulphate type, and is relatively high in Mg (Table 3). Temperature, DIC, Ca, and SO_4^{2-} all decrease downstream, whereas pH increases (Fig. 10). Unlike the Rembokola stream, there are no consistent changes in the concentrations of conservative elements (e.g. Cl^-).

Sinters, travertines and mixed deposits

The Rembokola sinters analysed in this study were dominated by opal-A, with more anhydrite-rich mineralogy in spicular facies. Layered sinter samples have elevated Al, Na and Ti compared to travertines (Table 4), reflecting a greater component of detrital clastic material (e.g. feldspar and magnetite, abundant in the volcanic host rocks) entrained within the sinter layers. The near-neutral to alkaline pH waters do not transport significant concentrations of Al or Ti, and Na is conserved in the aqueous phase and not readily precipitated. Sulphur is below detection limits in layered sinters, but relatively high (2.24 wt%) in the spicular sinters, confirming the presence of anhydrite in this facies. Sinter samples analysed by ICP-MS following aqua regia digestion (Table 5) show Te present in concentrations of 40 μg/kg, at least 800 times higher than in spring water (<0.05 μg/l), and ~8 times greater than average crustal abundances (Wedepohl 1995).

In the interlayered mixed, silica–carbonate deposit from Rembokola (SV482), Sr is high due to calcite contents (Table 4). Carbonate layers show significant arsenic enrichments compared to sinters and silica layers. Tellurium (Table 5) is higher in the bulk-analysed mixed sample than the sinters from the same stream, at concentrations >50 times higher than average crustal abundance (Wedepohl 1995).

All bulk Rembokola samples analysed in this study for elements related to epithermal mineralisation have low but significant concentrations of Au, Ag, Hg and Cu, as well as the Te previously discussed (Table 5).

The hot spring deposits of the Poghorovorughala area also have mixed mineralogy. Similar to the Rembokola sinters, Te contents of the deposits are high (250–380 μg/kg; Table 5) and spring waters are below detection limits (<0.05 μg/l). Lobate mixed silica–carbonate samples show elevated Al and Ti in a similar fashion to the layered sinters of Rembokola (Table 4), most likely representing detrital or substrate material entrained within the sample (e.g. Fig. 6B).

The travertine deposits of Tanginakulu are dominated by calcite. Similar to the mixed samples from Rembokola and Poghorovorughala, Te occurs in very high concentrations (410 μg/kg; Table 5). Tanginakulu travertines contain notably high Fe concentrations; springs in the area deposit distinctly red sediments (sludge) upon discharge, probably indicative of reduced waters being oxidised upon exiting at the surface.

Discussion

Travertines and travertine-forming waters

Tanginakulu stream is dominated by relatively cool Ca–Mg–HCO_3^- type water compositions. The magnesium contents indicate a low temperature (<100°C) origin for these waters, as at higher temperatures Mg is readily removed by formation of minerals such as chlorite (Giggenbach 1988). Stream waters are moderately supersaturated with respect to calcite (Fig. 10), with log Q/K = 0.5 to 1, where Q is the ion activity product and K is the equilibrium constant of the calcite-forming reaction, as calculated with SOLVEQ (Reed 1982; 1998). The Tanginakulu spring analysed in this study has values of log Q/K = −0.3.

Travertine precipitation from stream and spring waters initially enriched with calcium and bicarbonate is typically driven by CO_2 removal (Pentecost 2003):

$$Ca^{2+} + 2HCO_3^- = H_2O + CaCO_3 + CO_2 \qquad \mathbf{1}$$

Removal of carbon dioxide can be biotic (photosynthesis), or abiotic (degassing). The latter mechanism is the predominant process in most streams and springs, and is particularly effective where water is turbulent (Pentecost 2003). There is a strong association with travertine deposition and thicker deposits in areas of waterfalls and rapids on Savo. Carbon

dioxide loss to the atmosphere is therefore the most likely cause of calcite supersaturation and precipitation.

Examination of travertines (Fig. 8) shows that they are composed of layers of calcite ray-crystals. Calcite is the dominant $CaCO_3$ polymorph at temperatures <40°C (Jones *et al.* 1996), and so its predominance over aragonite in these deposits is unsurprising. Ray-crystal layers are common in travertine, and are typically abiotic in origin, formed by rapid precipitation of calcite from supersaturated solutions (Folk *et al.* 1985; Chafetz & Guidry 1999).

As well as causing carbonate precipitation, CO_2 loss is an important mechanism for increasing water pH (Chafetz *et al.* 1991; Fouke *et al.* 2000):

$$HCO_3^- + H^+ = H_2O + CO_2 \qquad \mathbf{2}$$

Figure 10 shows the changes in DIC and pH in the downstream direction of Tanginakulu stream. In particular, there is a rapid drop in DIC and corresponding increase in pH after discharge from the warm spring into the stream proper. Combined CO_2 loss and travertine precipitation is capable of producing the relationships displayed in figure 10.

Tellurium is notably enriched in carbonate bearing samples (Table 5), despite being below detection limit (<0.05 μg/l) in all water samples in this study. Arsenic also shows high concentrations in carbonates, particularly those within the mixed sample from Rembokola. Arsenic is associated with the higher temperature component: its concentration is higher in the Rembokola springs and stream than in the Ca–Mg–HCO_3^- enriched springs (Tables 2 and 3). Tellurium would also be expected to be associated with high temperature fluids, given that it can be transported in a magmatic vapour phase (Cooke *et al.* 1996). High Te concentrations in the carbonates may reflect tellurate substitution for CO_3^{2-}, in a similar mechanism to sulphate substitution (Takano *et al.* 1980). Elevated arsenic in carbonates likely reflects adsorption or co-precipitation of arsenate with calcite (Alexandratos *et al.* 2007). Thus, high concentrations of arsenic and tellurium occur in carbonate deposits – despite these deposits being associated with lower temperature fluids –as carbonate minerals are suitable hosts for As and Te. It appears that in the case of Rembokola, opal-A is less capable of hosting As and Te, despite being associated with the high temperature fluid end-member.

Sinters

Sinter is deposited within the Rembokola valley. The stream is a relatively closed system: there are few major springs feeding the stream other than those of the upstream thermal area, and there are no major tributaries into the stream. In the downstream direction, evaporation causes a decrease in temperature, and increases in conservative elements such as B, Li, and Cl^-. Simple calculations indicate that approximately 10% of the original mass of water is lost over <1 km to produce the observed Cl^- and Li increases. Mn and Si decrease by mineral precipitation, whereas CO_2 loss leads to pH increase (Eqn. 2) and DIC decrease (Fig. 9 and Table 2).

The combined effects of evaporation, cooling and CO_2 loss is that amorphous silica (opal-A) becomes increasingly supersaturated (increasing log Q/K) downstream (Fig. 9). Calcite is also supersaturated (decreasing downstream, due to decreasing temperature and retrograde calcite solubility; Rimstidt 1997) but the DIC contents of the waters are low (<50 mg/l HCO_3^- eqv.), and it is likely that any precipitated carbonate is masked by greater volumes of silica.

Silica precipitates near hot springs in two distinct facies – as terraced deposits on the steep slopes in the upper Rembokola valley, and as spicules on subaerially exposed substrate in the relatively flat-lying thermal area. The spiculose sinter described in this study is morphologically similar to the silica–carbonate “meringue” deposits of the Pavlova Spring, Ngatamariki, New Zealand (Campbell *et al.* 2002). These authors concluded that the Pavlova deposits formed by evaporation of hot spring-derived water from subaerially exposed surfaces, typically upon partially submerged detritus (principally leaf litter). Meniscoid and capillary creep ("wicking"; Hinman & Lindstrom 1996; Campbell *et al.* 2002), as well as sporadic bathing and splashing in the case of the Savo deposits, replenish fluids. Individual spicules reach a maximum height (~2 cm) above which the wicking process can no longer replenish moisture in sufficient quantity to allow further growth (Campbell *et al.* 2002). Further evidence of evaporation as a precipitation mechanism is the presence of anhydrite on the upper surfaces of the spicules (Fig. 3). At spring temperatures and below, anhydrite is undersaturated (Fig. 9). The only effective mechanism for precipitating anhydrite is evaporation.

The upstream terraced sinter may also be precipitated through evaporation, but in the case of the deposits on the steep slopes, wicking is less important than direct evaporation from the

surface. Water and dissolved silica is supplied constantly by the spring fluids bathing the discharge apron, whilst never submerging it entirely. Terrace-type constructions are common in both travertine and siliceous sinter deposits, and occur where precipitation is from sheet flow (Guidry & Chafetz 2003). The stair-step morphology of the micro-terracettes is produced by random perturbations in deposition, perhaps produced by debris or microbial mats (Chafetz & Folk 1984; Guidry & Chafetz 2003) that eventually reorganise into linear or curvilinear ridges (Hammer *et al.* 2007).

Evaporation and cooling of the hot spring fluids as they flow downstream leads to an increase in the saturation index of amorphous silica (Fig. 9) and sinter precipitation (Rimstidt & Cole 1983). Around hot springs, sinter only forms upon exposed or periodically bathed surfaces, but in the stream channel downstream of the hot springs, sinter is deposited upon wholly submerged surfaces. The sinters also contain filaments or tubules preserved by opal-A, typically aligned and orthogonal to the growth laminations of the sinter (Fig. 4). The orientation may be a result of filaments aligning with flow direction in the stream (Jones *et al.* 2003). Such filamentous structures are commonplace in siliceous sinters, and are the result of the enclosure and partial preservation of microbes (Jones & Renaut 2003a, b; Jones *et al.* 2003; Lynne & Campbell 2003; Konhauser *et al.* 2004; Fernandez-Turiel *et al.* 2005; Jones *et al.* 2005). Filaments were not observed in the spicular facies, and only rarely in the terraced sinter (Fig. 2); as the samples were not preserved with a fixative solution, the presence and abundance of microbes in these facies is unknown.

Thermal waters may be colonised by a range of microorganisms, including cyanobacteria, bacteria and fungi; however, low preservation fidelity of the organisms following silicification (replacement and/or encasement with silica, during or shortly after life) often makes taxonomic identification difficult (Jones *et al.* 2003). The fossils preserved in the Rembokola stream sinters are simple, non-branching filaments, approximately 100 µm in length and 5 µm in diameter, although silica cementation means that the diameter of the preserved filament may be significantly larger than that of the living organism, (Jones *et al.* 2003). *Phormidium* cyanobacteria are common in thermal areas, and have an appropriate morphology (Pentecost 2003) but the lack of more complex features preserved in the Rembokola sinters preclude definitive classification.

Some noteworthy aspects of the analysed sinter chemistry is the low but significant As concentrations, and 2–20 mg/kg Cu (Table 4, 5). Despite the Cu and Fe contents of the samples, no sulphide minerals (pyrite, chalcopyrite) were observed under SEM; in fact, with

the exception of anhydrite in the spicular and terraced sinter and a few clasts of detrital material (trachytic volcaniclasticswith elevated Al, Na and Ti; Table 4), no minerals other than opal-A were observed. Accessory elements can be bound into the structure of opal-A without requiring distinct mineral phases (Jones & Renaut 2003a). ICP-MS analysis of a subset of the sinter samples (Table 5) show that Te is lower than in carbonate samples, possibly reflecting more effective Te scavenging from fluids by carbonate than amorphous silica, as discussed above for the travertine samples.

Lobate and spicular mixed deposits

Mixed silica–carbonate + anhydrite spicules grow on the periphery of Poghorovorughala hot springs, upon infrequently splashed and bathed surfaces (Fig. 6A). The increased proportion of opal-A and anhydrite in these samples indicates that they precipitate from more highly evaporated spring waters, as anhydrite and amorphous silica are marginally saturated and undersaturated, respectively, in the spring waters. The spicules here are morphologically similar to those of the Rembokola area, albeit with more carbonate. Mineralogy is closer to the Pavlova Spring deposits (Campbell *et al.* 2002), with both carbonate and silica phases, and the spicules at Poghorovorughala are interpreted to form in the same way – by wicking of hydrothermal fluids from infrequently bathed and splashed surfaces, resulting in evaporative precipitation of sinter/travertine.

The lobate silica–carbonate deposits surrounding Poghorovorughala hot springs (Fig. 6) contain carbonates, with anhydrite and opal-A. In these deposits, CO_2 loss causes carbonate precipitation, and evaporation precipitates anhydrite and silica, similar to the spiculose facies. For the most part, deposits are microcrystalline to amorphous, with the exception of well-developed trigonal prisms of calcite in sheltered areas between lobes (Fig. 6H). At precipitation temperatures above 40°C, aragonite is the expected polymorph of $CaCO_3$, with some exceptions. For example, Jones *et al.* (1996) described calcite deposited from Waikite Hot Springs, New Zealand, where water temperatures are >90°C. The near-spring deposits at Poghorovorughala contain both calcite and aragonite, and water temperatures are >90°C; however, as the deposits are formed in splashed and bathed areas, rather than submerged, it is possible that there is precipitation both above *and* below the 40°C boundary temperature. Without real-time observations of precipitation it is difficult to determine whether calcite is precipitating at an unusually high temperature.

Interlayered mixed deposits

Interlayered mixed silica–carbonate deposits are found above present stream levels in the mid- to upper reaches of the Rembokola. The mixed deposits are clearly older than the silica sinters, as they are above the present day stream level, and have indurated and weathered upper surfaces (Fig. 5A). The silica layers include filaments in void spaces, similar to those observed in the stream sinters (Fig. 4E; Fig. 5E). The silica layers tend to be more massive than in the silica-only sinters, with fewer preserved filaments and lower porosity, perhaps as a function of age. Over time, diagenetic transformation and continued silica precipitation leads to the destruction of primary depositional fabrics (Jones & Renaut 2003a). As discussed above, silica layers tend to have a higher clastic content than carbonate layers (Fig. 5F).

Carbonate layers in the Rembokola mixed deposit consist of ray-crystal calcite (Fig. 5C), similar to the travertines at Tanginakulu. Similar precipitation mechanisms are envisaged – CO_2 degassing in an area of turbulent flow leads to calcite supersaturation and precipitation. SV482 in particular shows enrichments of Te and As, both considered pathfinder elements for epithermal Au deposits (White & Hedenquist 1995), with Te in particular associated with alkaline-related epithermal deposits (Jensen & Barton 2000). The increased concentration of Te and As in SV482 relative to Rembokola sinters is potentially a result of the combination of more effective scavenging of these elements by carbonates. SV482 also has higher As and Te than travertine from Tanginakulu, potentially reflecting increased concentration of these elements in the waters forming mixed deposits versus those that only form travertine.

Interlayered mixed silica–carbonate deposits are also found surrounding the Mound Spring at Poghorovorughala (Fig. 7). Layers of opal-A contain filaments similar to the sinters elsewhere on the island (Fig. 7D; Fig. 4D). The lack of alignment in the filaments is most likely a result of the low flow rate on the Mound Spring's discharge apron relative to the Rembokola stream.

Although elsewhere calcite and silica can be found in the same deposits, (Jones *et al.* 1996; Campbell *et al.* 2002), the situation is rare, as the two minerals are associated with different fluid types (in terms of origin and chemistry) in most geothermal areas (Canet *et al.* 2005). The interlayered silica–carbonate deposits show that the Rembokola stream and Poghorovorughala Mound Spring have historically alternated between travertine and sinter formation. Carbonate precipitation is from waters with a higher contribution from low-temperature fluid (e.g. Tanginakulu bicarbonate-sulphate spring), and silica precipitation is

from waters dominated by the higher temperature fluids. The periodic switching between the two situations reflects changes in the degree of mixing between the two end-member fluids at source. If DIC contents are too low, then calcite precipitation is masked by silica precipitation, or simply prohibited by the lack of sufficient supersaturation.

Comparison between the Rembokola and Poghorovorughala springs shows that fluid mixing already occurs (Smith *et al.* 2010); for example, Mg contents are far higher than would be expected for waters at the temperatures recorded (Giggenbach 1988). The Poghorovorughala springs have a higher contribution from the Ca–Mg–HCO_3^- end-member compared to the Rembokola springs. Poghorovorughala spring waters are supersaturated with a number of mineral phases at discharge temperature, most notably with calcite ($\log Q/K \approx 1.2$), and aragonite ($\log Q/K \approx 1.1$), and saturated with anhydrite ($\log Q/K \approx 0.1$). The waters are under-saturated with respect to amorphous silica ($\log Q/K \approx -0.2$) although should saturate upon cooling to approximately 60°C (calculated with SOLVEQ; Reed 1982; Reed 1998). At present, the Rembokola waters precipitate only opal-A (and minor anhydrite) whereas the Poghorovorughala springs precipitate carbonates, opal-A and anhydrite.

What causes the periodic changeover between carbonate and silica precipitation in interlayered mixed samples is unknown. Three principal mechanisms can be suggested: 1) episodic changes in relative contribution of magmatic fluids to the hydrothermal system (Boichu *et al.* 2008); 2) changes in the hydrology and plumbing of the system causing varying contributions of both components (e.g. Leeman *et al.* 2005); 3) seasonal changes in rainfall causing variation in the low temperature components (e.g. López *et al.* 2006). All three models may operate to produce periodic changes in the hydrothermal system at Savo; indeed, López *et al.* (2006) point out that there may be relationships between the different mechanisms, such as atmospheric pressure affecting rainfall, degassing rate and seismic tremor (López *et al.* 2006; Neuberg 2000). Irrespective of the mechanism driving periodic switchover between carbonate and silica in interlayered mixed samples, the importance of high meteoric water input to the hydrothermal system of Savo is underlined, as it is the mixing of the meteoric-derived low temperature end-member that drives hot springs and streams from silica to carbonate precipitation.

Conclusions

Hydrothermal discharges at Savo produce a range of deposits, including travertine, sinter and unusual mixed silica–carbonate rocks. Previous work has shown that there are multiple fluid

types within the hydrothermal system, including a silica-rich end-member associated with high temperature water–rock–gas interaction, and a Ca–Mg–HCO_3^- end-member derived by low temperature water–rock–gas interaction. The streams and springs discussed in this study can be classified according to which component dominates: Rembokola is dominated by the high-temperature end-member, Tanginakulu by the low-temperature end-member, and Poghorovorughala springs are mixed.

The different water chemistries of the springs and their outflow streams give rise to different surface deposits. Waters dominated by the Ca–Mg–HCO_3^- end-member precipitate travertine, those dominated by the high-temperature end-member form silica sinter, and the Poghorovorughala springs form intimately mixed silica–carbonate lobes and spicules.

Unusual interlayered mixed silica–carbonate deposits occur in the Rembokola stream system and surrounding the Mound Spring at Poghorovorughala. The carbonate layers are similar to the travertine found in the Tanginakulu area, and the silica layers similar to the sinters currently forming in the Rembokola stream. The samples may reflect meteorological changes, possibly seasonal, with high rainfall leading to increased contributions from a low temperature, carbonate-forming, fluid end-member. Periodic changes in magma degassing, and reorganisations of the hydrothermal plumbing system by seismic activity may also account for the periodic variations in spring discharges and their products.

The Savo deposits show that sinter and travertine can be deposited from the same spring with relatively little change in water chemistry required, only a change in the relative contributions of two end-member fluids. As a result, travertines – normally associated with fluids peripheral to a hydrothermal system – can carry chemical signatures (e.g. enriched Te) more usually associated with sinter-forming, higher temperature, ‘hypogene’ fluids fed by magmatic volatiles. In particular, the carbonate layers of the mixed silica–carbonate deposits record high As and Te concentrations. This reflects the increased availability of these magmatic-hydrothermal components in the high temperature end-member fluid, combined with adsorption of arsenate and tellurate species by carbonate minerals.

In magmatic-hydrothermal systems with considerable meteoric water input, cooler-water deposits, i.e. travertine, are favoured. As such, travertine, and in particular, mixed silica–carbonate deposits can carry trace elements indicative of the underlying magmatic-hydrothermal system, pointing to potential economic mineralisation at depth.

Acknowledgements

DJS was funded by the Natural Environment Research Council (UK) and British Geological Survey University Funding Initiative as part of PhD studentship NER/S/A/2004/12339. SF received funding from the Society of Economic Geologists Student Research Grants (Hugh E. McKinstry Award). The authors would like to thank H. Taylor, K. Green and RA. Shaw (BGS); W. Satokana, G. Albert, A. Ramo, D. Billy and S. Basi (Solomon Islands Geology Division). JN and SRNC publish with the permission of the Executive Director, British Geological Survey (NERC). This paper is dedicated to the late Watson Satokana – without him this project would not have been possible.

References

ALEXANDRATOS, V.G., ELZINGA, E.J., and REEDER, R.J. 2007. Arsenate uptake by calcite: Macroscopic and spectroscopic characterization of adsorption and incorporation mechanisms. *Geochimica et Cosmochimica Acta*, **71**, 4172–4187.

BOICHU, M., VILLEMANT, B., and BOUDON, G. 2008. A model for episodic degassing of an andesitic magma intrusion. *Journal of Geophysical Research*, **113**, B07202.

CABON, J.Y. & CABON, N. 2000. Determination of arsenic species in seawater by flow injection hydride generation in situ collection followed by graphite furnace atomic absorption spectrometry: Stability of As(III). *Analytica Chimica Acta*, **418**, 19–31.

CAMPBELL, K.A., RODGERS, K.A., BROTHERIDGE, J.M.A., and BROWNE, P.R.L. 2002. An unusual modern silica-carbonate sinter from Pavlova spring, Ngatamariki, New Zealand. *Sedimentology*, **49**, 835–854.

CANET, C., PROL-LEDESMA, R.M., TORRES-ALVARADO, I., GILG, H.A., VILLANUEVA, R.E., and CRUZ, R.L.-S. 2005. Silica-carbonate stromatolites related to coastal hydrothermal venting in Bahía Concepción, Baja California Sur, Mexico. *Sedimentary Geology*, **174**, 97–113.

CHAFETZ, H.S. & FOLK, R.L. 1984. Travertines; depositional morphology and the bacterially constructed constituents *Journal of Sedimentary Research*, **54**, 289–316.

CHAFETZ, H.S. & GUIDRY, S.A. 1999. Bacterial shrubs, crystal shrubs, and ray-crystal shrubs: bacterial vs. abiotic precipitation. *Sedimentary Geology*, **126**, 57–74.

CHAFETZ, H.S., RUSH, P.F., and UTECH, N.M. 1991. Microenvironmental controls on mineralogy and habit of $CaCO_3$ precipitates: an example from an active travertine system. *Sedimentology*, **38**, 107–126.

CARMAN, G.D., 2003, Geology, mineralization and hydrothermal evolution of the Ladolam gold deposit, Lihir Island, Papua New Guinea, *In* SIMMONS, S.F., and GRAHAM, I., (eds), *Volcanic, Geothermal and Ore-Forming Fluids: Rulers and Witnesses of Processes within the Earth.*Society of Economic Geologists, Littleton, Colorado, *Special Publication No. 10*, 247–284.

COOKE, D.R., MCPHAIL, D.C., and BLOOM, M.S. 1996. Epithermal gold mineralization, Acupan, Baguio district, Philippines: Geology, mineralization, alteration and the thermochemical environment of ore deposition. *Economic Geology*, **91**, 243–272.

FARMER, J.D. 2000. Hydrothermal systems: doorways to early biosphere evolution. *GSA Today*, **10**, 2-9

FERNANDEZ-TURIEL, J.L., GARCIA-VALLES, M., GIMENO-TORRENTE, D., SAAVEDRA-ALONSO, J., and MARTINEZ-MANENT, S. 2005. The hot spring and geyser sinters of El Tatio, Northern Chile. *Sedimentary Geology*, **180**, 125–147.

FOLK, R.L., CHAFETZ, H.S., and TIEZZI, P.A., 1985. Bizarre forms of depositional and diagenetic calcite in hot spring travertine, central Italy, *In* SCHNEIDERMANN, N., and HARRIS, P.M., (eds), *Carbonate Cements.*Society of Economic Paleontologists and Mineralogists, Special Publication 36, 349–369.

FOUKE, B.W., FARMER, J.D., DES MARAIS, D.J., PRATT, L., STURCHIO, N.C., BURNS, P.C., and DISCIPULO, M.K. 2000. Depositional Facies and Aqueous-Solid Geochemistry of Travertine-Depositing Hot Springs (Angel Terrace, Mammoth Hot Springs, Yellowstone National Park, U.S.A.). *Journal of Sedimentary Research*, **70**, 565–585.

FOURNIER, R.O. & ROWE, J.J., 1966. Estimation of underground temperatures form silica content of water from hot springs and wet-steam wells. *American Journal of Science* **264**, 685–697.

512 GIGGENBACH, W.F. 1988. Geothermal solute equilibria: Derivation of Na-K-Mg-Ca geoindicators. *Geochimica*
513 *et Cosmochimica Acta*, **52**, 2749–2765.
514 GUIDRY, S.A. & CHAFETZ, H.S. 2003. Anatomy of siliceous hot springs: examples from Yellowstone National
515 Park, Wyoming, USA. *Sedimentary Geology*, **157**, 71–106.
516 HAMMER, Ø., DYSTHE, D.K., and JAMTVEIT, B. 2007. The dynamics of travertine dams. *Earth and Planetary*
517 *Science Letters*, **256**, 258–263.
518 HEDENQUIST, J.W., ARRIBAS, A.R., and GONZALEZ-URIEN, E., 2000, Exploration for epithermal gold deposits,
519 *In* HAGEMANN, S.G., and BROWN, P.E., (eds), *Gold in 2000*.Society of Economic Geologists, Littleton,
520 Colorado, *Reviews in Economic Geology* **13**, 245–277.
521 HINMAN, N.W. & LINDSTROM, R.F. 1996. Seasonal changes in silica deposition in hot spring systems. *Chemical*
522 *Geology*, **132**, 237–246.
523 JENSEN, E.P. & BARTON, M.D., 2000, Gold deposits related to alkaline magmatism, *In* HAGEMANN, S.G., and
524 BROWN, P.E., (eds), *Gold in 2000*.Society of Economic Geologists, Littleton, Colorado, *Review in*
525 *Economic Geology* **13**, 279–314.
526 JONES, B. & RENAUT, R.W. 2003a. Hot spring and geyser sinters: the integrated product of precipitation,
527 replacement, and deposition. *Canadian Journal of Earth Sciences*, **40**, 1549–1569.
528 JONES, B. & RENAUT, R.W. 2003b. Petrography and genesis of spicular and columnar geyserite from the
529 Whakarewarewa and Orakeikorako geothermal areas, North Island, New Zealand. *Canadian Journal of*
530 *Earth Sciences*, **40**, 1585–1610.
531 JONES, B., RENAUT, R.W., and KONHAUSER, K.O. 2005. Genesis of large siliceous stromatolites at Frying Pan
532 Lake, Waimangu geothermal field, North Island, New Zealand. *Sedimentology*, **52**, 1229–1252.
533 JONES, B., RENAUT, R.W., and ROSEN, M.R. 1996. High-temperature (>90°C) calcite precipitation at Waikite
534 Hot Springs, North Island, New Zealand. *Journal of the Geological Society*, **153**, 481–496.
535 JONES, B., RENAUT, R.W., and ROSEN, M.R. 2003. Taxonomic fidelity of silicified filamentous microbes from
536 hot-spring systems in the Taupo Volcanic Zone, North Island, New Zealand. *Transactions of the Royal*
537 *Society of Edinburgh: Earth Sciences*, **94**, 475–483.
538 KONHAUSER, K.O., JONES, B., PHOENIX, V.R., FERRIS, G., and RENAUT, R.W. 2004. A model for hot spring
539 silicification. *Ambio*, **33**, 552–558.
540 LEEMAN, W.P., TONARINI, S., PENNISI, M., and FERRARA, G. 2005. Boron isotopic variations in fumarolic
541 condensates and thermal waters from Vulcano Island, Italy: Implications for evolution of volcanic
542 fluids. *Geochimica et Cosmochimica Acta*, **69**, 143–163.
543 LÓPEZ, D.L., BUNDSCHUH, J., SOTO, G.J., FERNÁNDEZ, J.F., and ALVARADO, G.E. 2006. Chemical evolution of
544 thermal springs at Arenal Volcano, Costa Rica: Effect of volcanic activity, precipitation, seismic
545 activity, and Earth tides. *Journal of Volcanology and Geothermal Research*, **157**, 166-181.
546 LYNNE, B.Y. & CAMPBELL, K.A. 2003. Diagenetic transformations (opal-A to quartz) of low- and mid-
547 temperature microbial textures in siliceous hot-spring deposits, Taupo Volcanic Zone, New Zealand.
548 *Canadian Journal of Earth Sciences*, **40**, 1679–1696.
549 NEUBERG, J. 2000. External modulation of volcanic activity. *Geophysical Journal International*, **142**, 232-240.
550 PENTECOST, A. 2003. Cyanobacteria associated with hot spring travertines. *Canadian Journal of Earth Sciences*,
551 **40**, 1447–1457.
552 PETTERSON, M.G., CRONIN, S.J., TAYLOR, P.W., TOLIA, D., PAPABATU, A., TOBA, T., and QOPOTO, C. 2003.
553 The eruptive history and volcanic hazards of Savo, Solomon Islands. *Bulletin of Volcanology*, **65**, 165–
554 181.
555 REED, M.H. 1982. Calculation of multicomponent chemical equilibria and reaction processes in systems
556 involving minerals, gases and an aqueous phase. *Geochimica et Cosmochimica Acta*, **46**, 513–528.
557 REED, M.H., 1998, Calculation of simultaneous chemical equilibria in aqueous-mineral-gas systems and its
558 application to modeling hydrothermal processes., *In* RICHARDS, J., and LARSON, P., (eds), *Techniques*
559 *in Hydrothermal Ore Deposits Geology*.Society of Economic Geologists, *Reviews in Economic*
560 *Geology* **10**, 109–124.
561 RENAUT, R.W. & JONES, B. 2003. Sedimentology of hot spring systems. *Canadian Journal of Earth Sciences*,
562 **40**, 1439–1442.
563 RIMSTIDT, J.D. & COLE, D.R. 1983. Geothermal mineralization; I, The mechanism of formation of the
564 Beowawe, Nevada, siliceous sinter deposit. *American Journal of Science*, **283**, 861–875.
565 RIMSTIDT, J.D. 1997. Gangue mineral transport and deposition, *In* BARNES H.L. (ed), *Geochemistry of*
566 *Hydrothermal Ore Deposits*, 3rd Edition, Wiley and Sons, 487–515
567 RODGERS, K.A., BROWNE, P.R.L., BUDDLE, T.F., COOK, K.L., GREATREX, R.A., HAMPTON, W.A., HERDIANITA,
568 N.R., HOLLAND, G.R., LYNNE, B.Y., MARTIN, R., NEWTON, Z., PASTARS, D., SANNAZARRO, K.L., and
569 TEECE, C.I.A. 2004. Silica phases in sinters and residues from geothermal fields of New Zealand.
570 *Earth-Science Reviews*, **66**, 1–61.

SCHINTEIE, R., CAMPBELL, K.A., AND BROWNE, P.R.L. 2007. Microfacies of Stromatolitic Sinter from Acid-sulphate-chloride Springs at Parariki Stream, Rotokawa Geothermal Field, New Zealand. *Palaeontologia Electronica*, **10**, 1.4A.

SMITH, D.J., JENKIN, G.R.T., NADEN, J., BOYCE, A.J., PETTERSON, M.G., TOBA, T., DARLING, W.G., TAYLOR, H., and MILLAR, I.L. 2010. Anomalous alkaline sulphate fluids produced in a magmatic hydrothermal system - Savo, Solomon Islands. *Chemical Geology*, **275**, 35–49.

SMITH, D.J., PETTERSON, M.G., SAUNDERS, A.D., MILLAR, I.L., JENKIN, G.R.T., TOBA, T., NADEN, J., and COOK, J.M. 2009. The petrogenesis of sodic island arc magmas at Savo volcano, Solomon Islands. *Contributions to Mineralogy and Petrology*, **158**, 785–801.

TAKANO, B., ASANO, Y., and WATANUKI, K. 1980. Characterization of sulfate ion in travertine. *Contributions to Mineralogy and Petrology*, **72**, 197-203.

UYSAL, I.T., GASPARON, M., BOLHAR, R., ZHAO, J.-X., FENG, Y.-X., and JONES, G. 2011. Trace element composition of near-surface silica deposits--A powerful tool for detecting hydrothermal mineral and energy resources. *Chemical Geology*, **280**, 154-169.

VIKRE, P.G. 2007. Sinter-Vein Correlations at Buckskin Mountain, National District, Humboldt County, Nevada. *Economic Geology*, **102**, 193–224.

WEDEPOHL, K.H. 1995. The composition of the continental crust. *Geochimica et Cosmochimica Acta*, **59**, 1217–1232.

WHITE, N.C. & HEDENQUIST, J.W. 1995. Epithermal gold deposits: styles, characteristics and exploration. *SEG Newsletter*, **23**, 1–13.

Figures

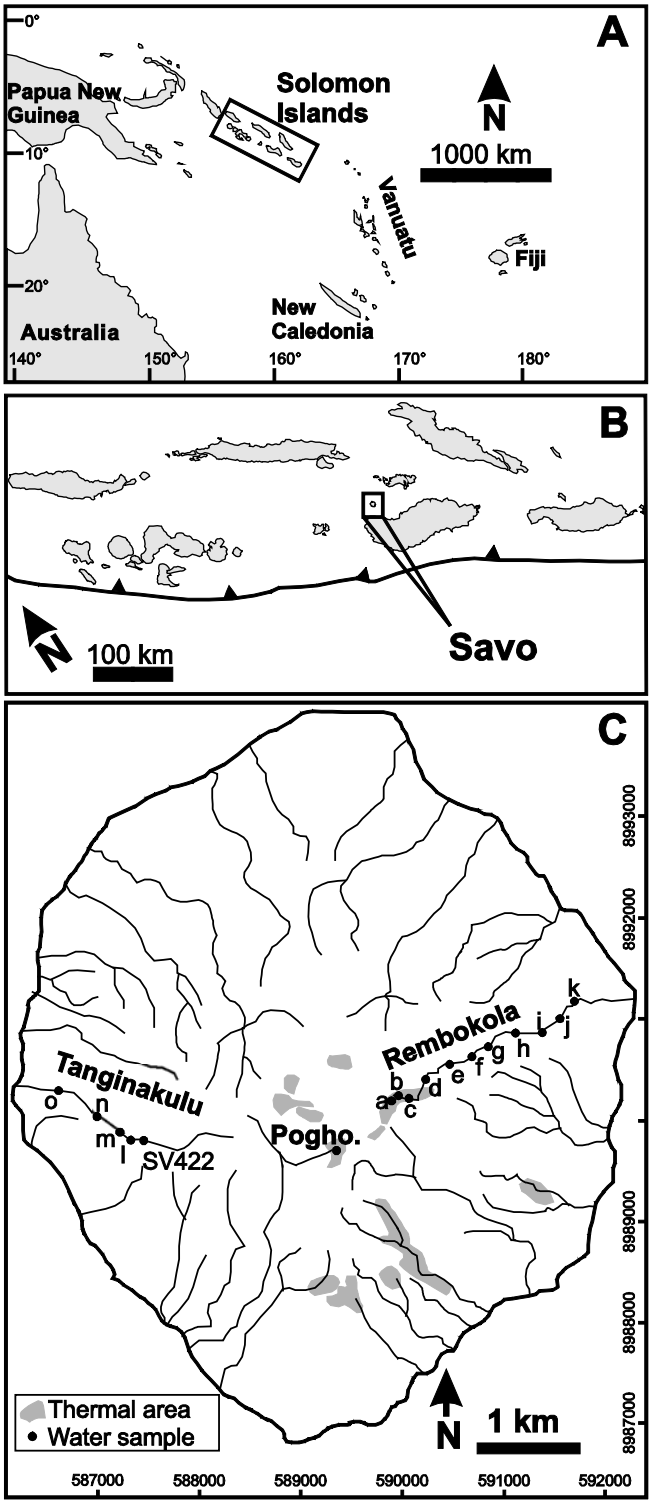

Fig. 1: A) Map of the south west Pacific. Solomon Islands shown in box. B) Map of the Solomon Islands, showing location of Savo. C) Map of Savo showing location of major streams, thermal areas, and water samples discussed in this study. Pogho. = Poghorovorughala.

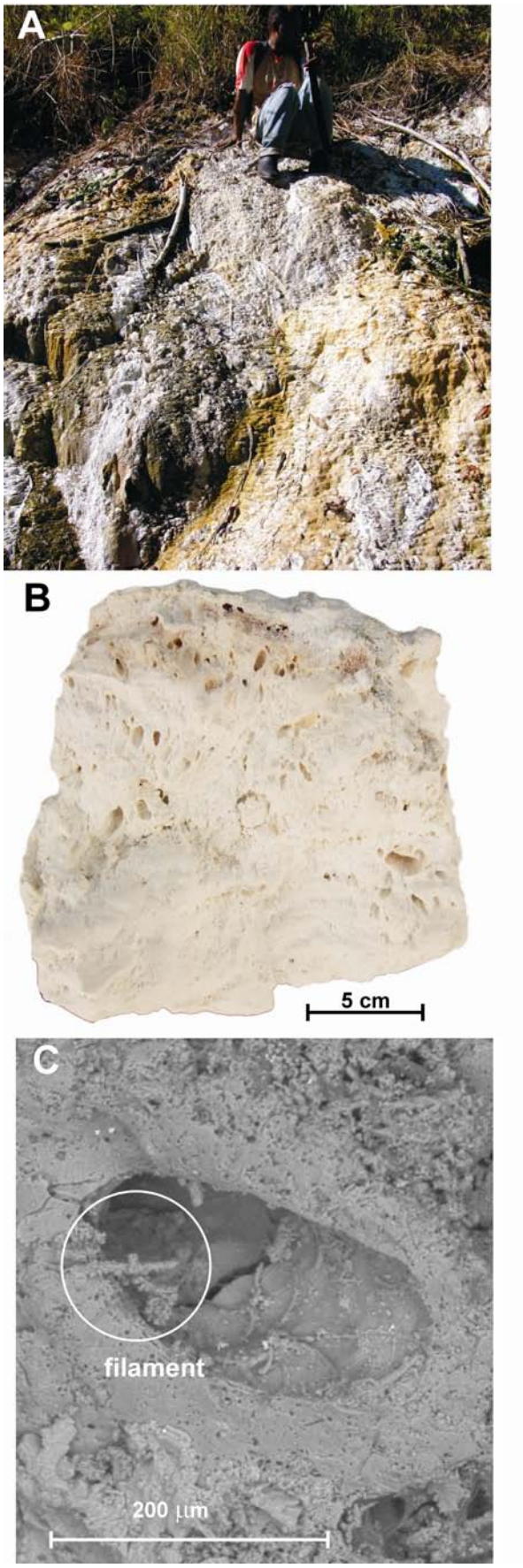

Fig. 2: Rembokola terraced sinter. A) Terraced sinter (east of point a, Fig. 1). Deposit is composed of micro-terracettes of opal-A. B) Photograph of the interior of the sinter, showing highly porous opal-A. C) BSE image of broken surface showing silica-encrusted filament in cavity.

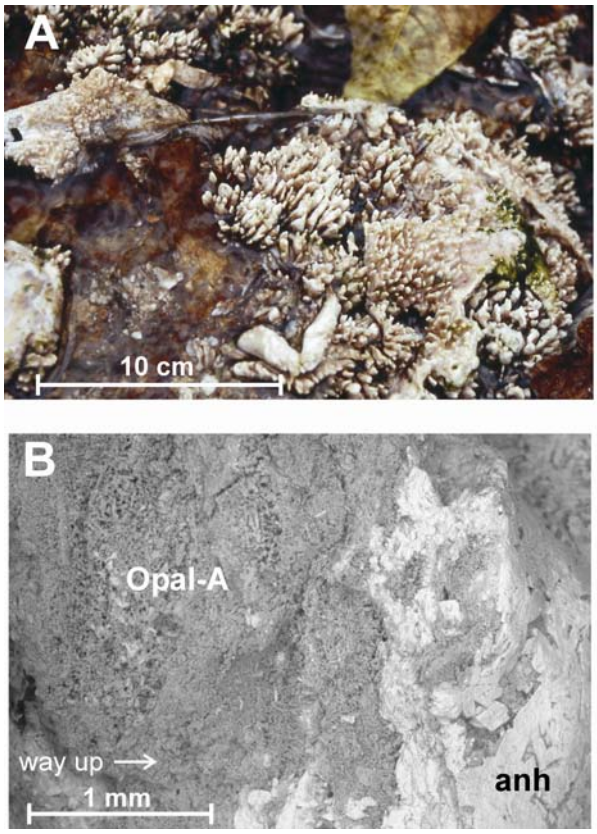

Fig. 3: Rembokola spicular sinter (points a and b, Fig. 1). A) Opal-A sinter growing on leaf litter in Rembokola stream, at Toakomata hot spring area. B) Back scattered electron (BSE) image of Rembokola spicular sinter. Upper surface is to the right in the field of view, and contains more anhydrite (white) than the lower areas, which is dominated by opal-A (grey).

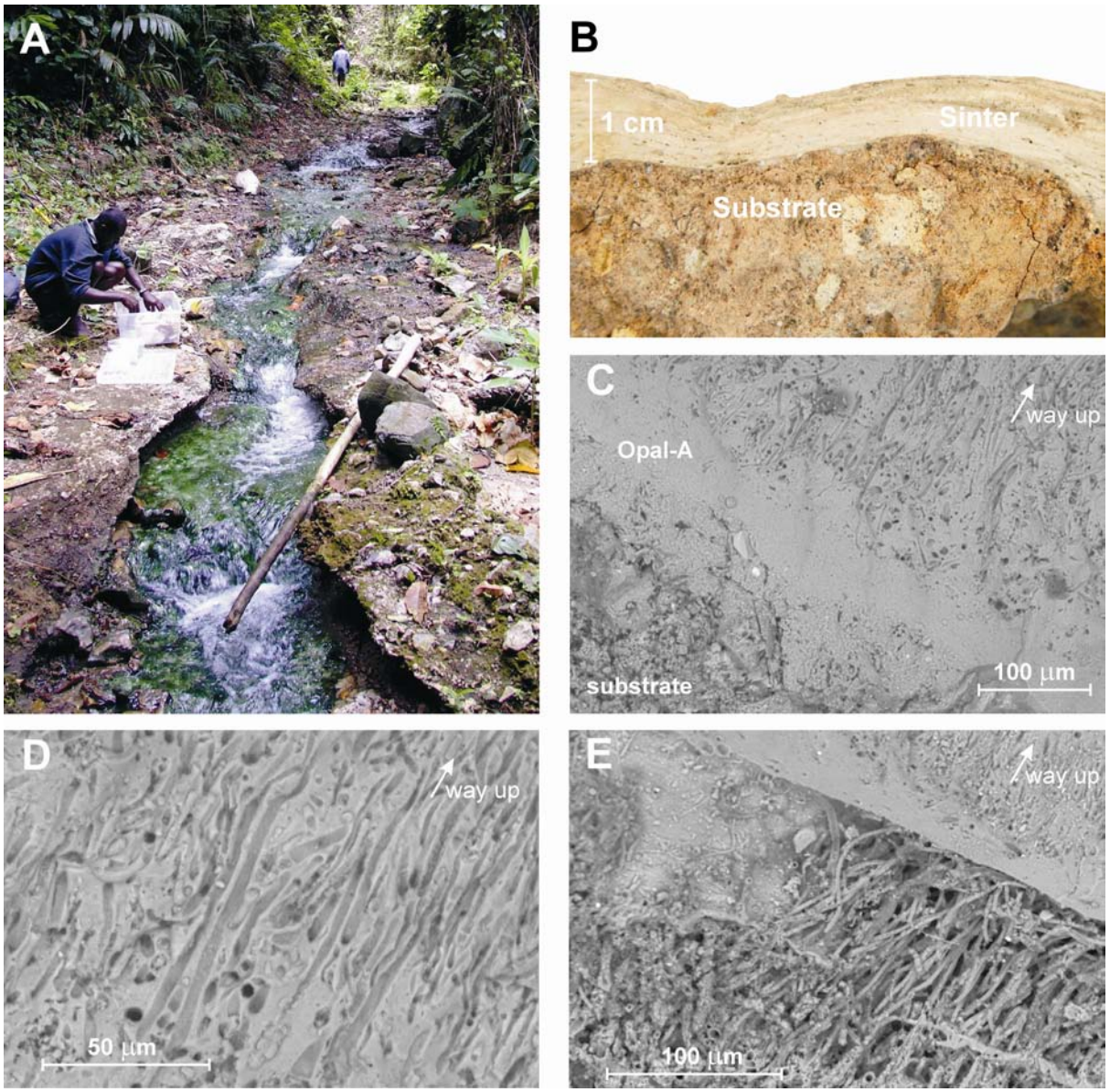

Fig. 4: Silica sinter in the Rembokola valley (point e, Fig. 1). A) Rembokola stream channel is lined with sinter (covered with algae in this view). The surrounding gorge floor is clastic material cemented by silica sinter. B) Cross section view through a silica sinter crust on sediment substrate. C) BSE image of broken surface showing laminations in sinter; lower layer is massive and low porosity opal-A, upper layer is more porous contains elongate filaments. D) BSE image of elongate hollow filaments in sinter. E) BSE image of filaments within a larger void space.

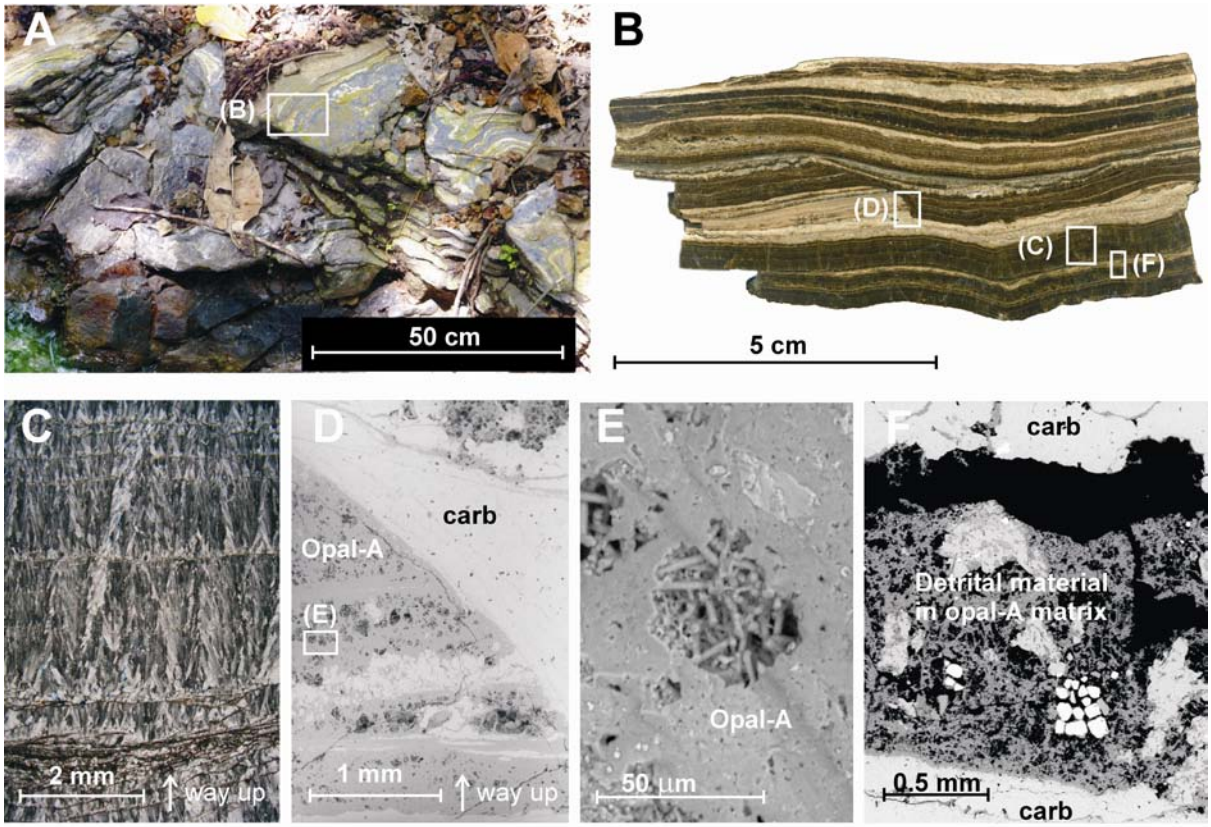

Fig. 5: Interlayered mixed silica–carbonate sinter, Rembokola valley (point d, Fig. 1). A) Terrace of mixed sinter approximately 30 cm above current stream water level. B) Cross section through sinter showing layers of calcite (dark) and opal-A (pale). C) Thin section through carbonate layers showing fans of ray-crystals (cross polarised light). D) BSE image showing calcite layer onlapping onto older silica and carbonate layers. E) BSE image of silica layer, with filaments visible in void space. F) BSE image from thin section showing silica layer with detrital material (white = magnetite, grey = feldspar, derived from local volcaniclastics). Carbonate layers (top and bottom of image) contain fewer clasts of foreign material.

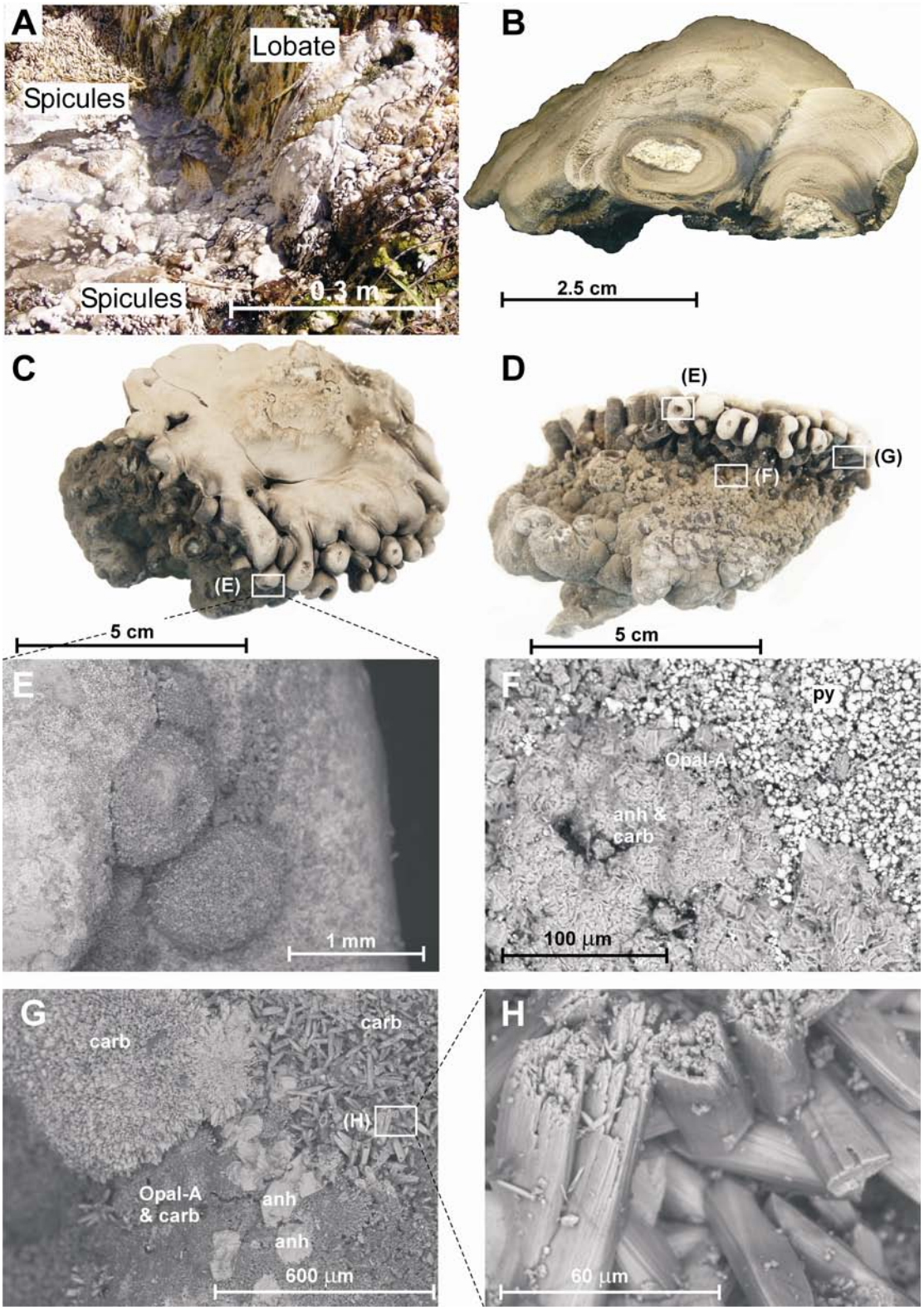

Fig. 6: Lobate deposits, Poghorovorughala. A) Lobate deposits surround the spring (visible as dark cavity immediately right of lobate label) and discharge channel; spicules occur on the periphery. B) Cross section through lobes, showing concentric laminations. Centre of lobe is kaolinite-dominated, representing the substrate of the steam-heated ground on which the deposits form. C) Upper surface of lobe. D) BSE image of underside of lobe (submerged portion). E) BSE image of rounded lobes of carbonate developing on subaerially exposed / splashed portion. F) BSE image of pyrite on surface of carbonate, opal-A and minor anhydrite in submerged portion. G) BSE image of carbonate and opal-A, with occasional anhydrite crystals, on splashed area of deposit. H) Detail view of calcite, showing trigonal crystal form.

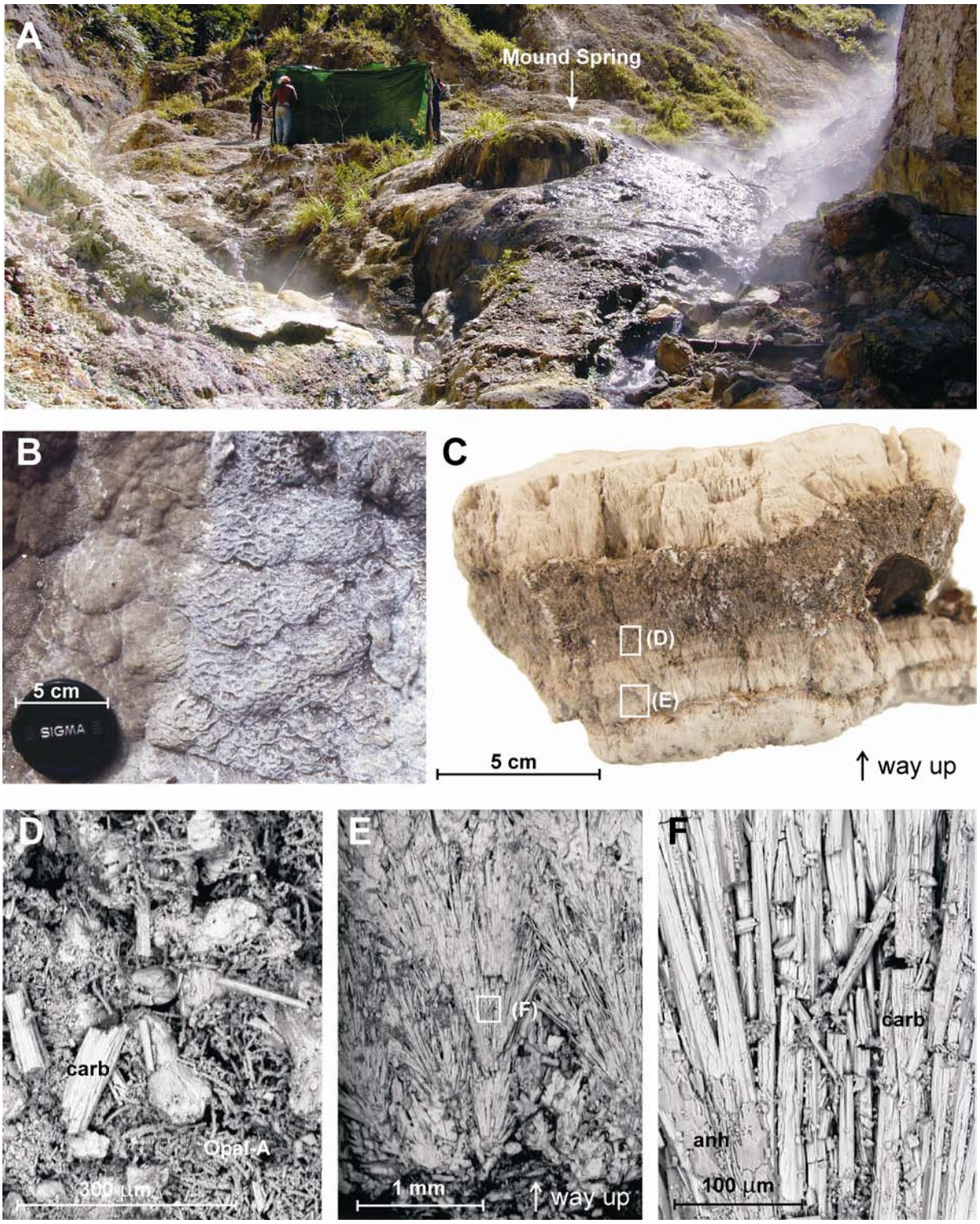

Fig. 7: Interlayered mixed silica–carbonate deposits, Poghorovorughala. A). View of Mound Spring, a 3 m high interlayered deposit of . A hot spring discharges from the summit of the mound. B) Micro-terracette texture on surface of the Mound Spring. C) Cross section through mixed layers of Mound Spring deposit. D) Dark layer is a mixture of tubes/ filaments of opal-A, and crystals of calcite, shown in BSE image. E) BSE image of carbonate fans from pale layers of mixed deposit. F) Detail view of calcite ray-crystals, showing minor anhydrite.

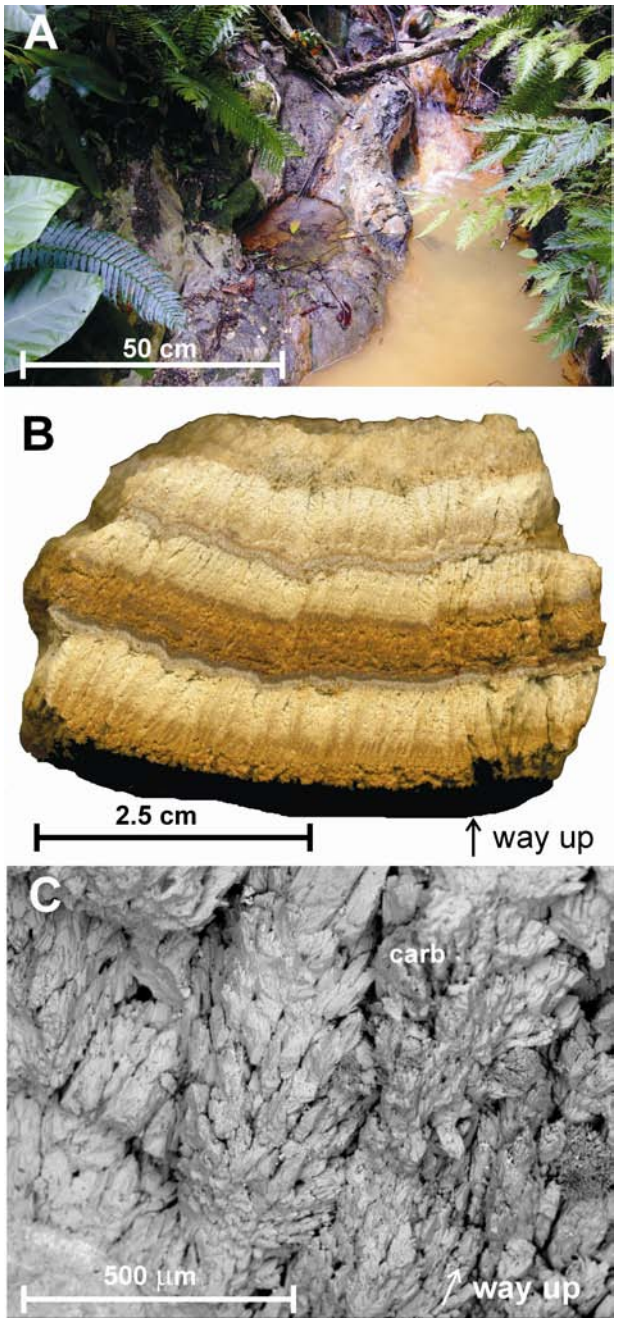

Fig. 8: Tanginakulu travertine deposits. A) Travertine deposited at small stream rapids. B & C) Cross section photograph and BSE image through travertine showing laminations of carbonate and fans of elongate calcite ray-crystals.

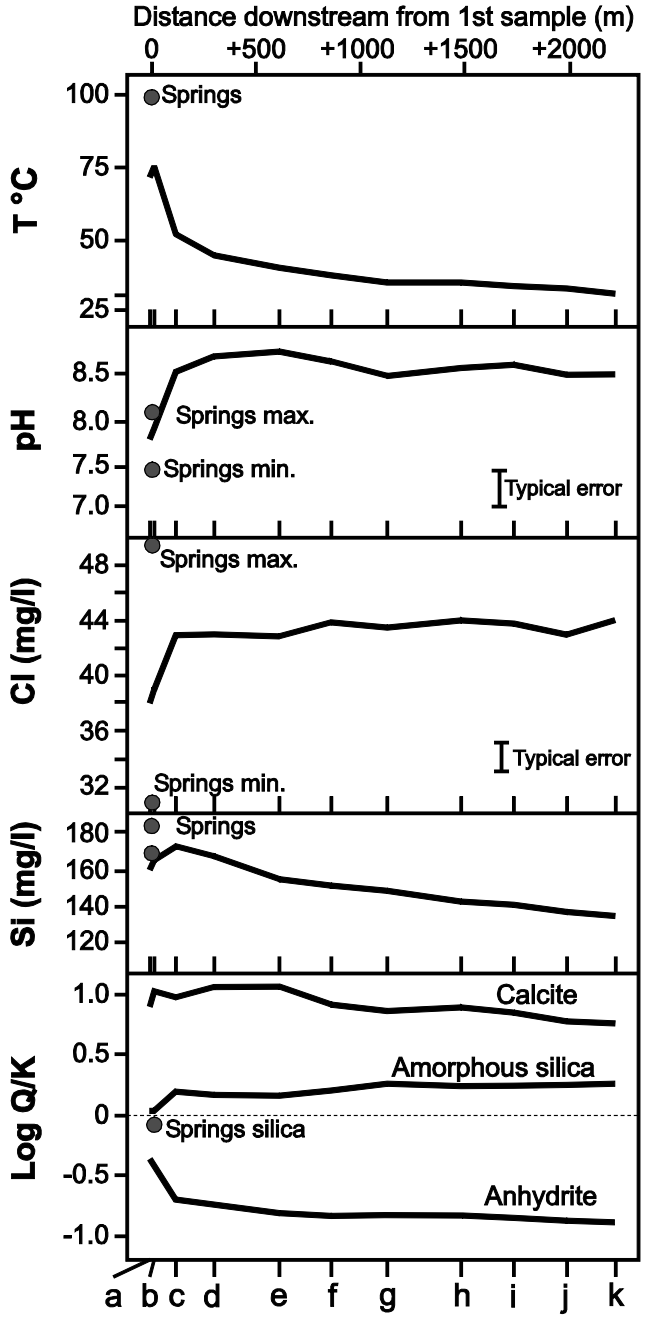

Fig. 9: Changes in temperature, pH, dissolved Cl and Si concentrations, and saturation index of important minerals in the Rembokola stream. Representative alkaline sulphate springs (or maximum and minimum values in the case of a range) shown for comparison. Error bars are ±1σ; not shown when within point size.

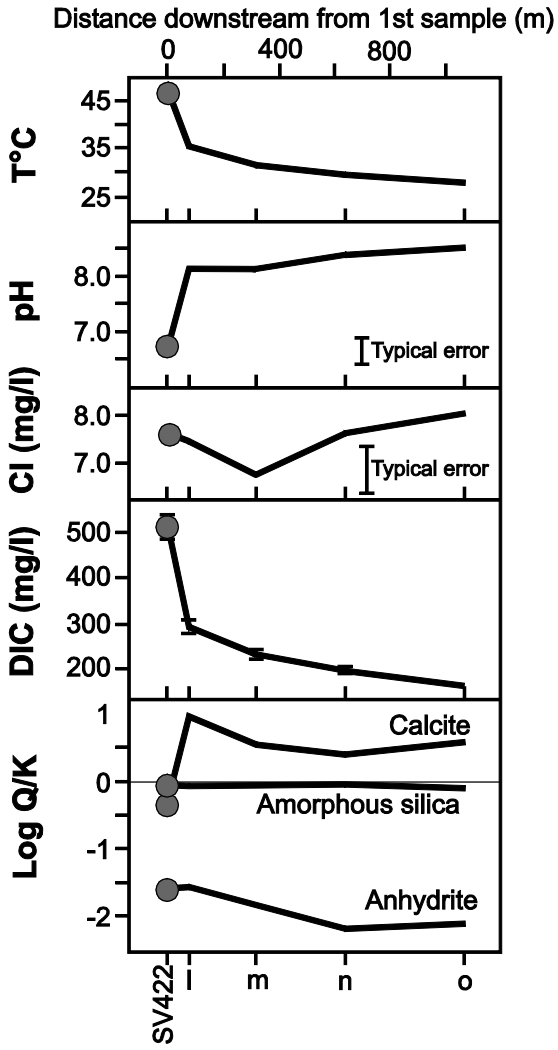

Fig. 10: Changes in temperature, pH, dissolved Cl, DIC (as HCO_3^- eqv.), and saturation index of important minerals in the Tanginakulu stream. SV422 is a warm spring in the upper reaches of the stream (Table 1). Error bars are ±1σ; not shown when within point size.

Tables

Table 1: Water chemistry from selected springs on Savo.

Sample	**Pogho. hot spring**	**Rembokola hot spring**	**Tanginakulu spring SV422**
Type	Alkaline sulphate	Alkaline sulphate	Bicarbonate sulphate
T (°C)	100	100	47
pH	7.5	7.5	6.7
Al (µg/l)	11	7	2
As (µg/l)	<2	50	19
B	2.15	8.78	0.20
Ba (µg/l)	40.9	55.8	44.3
Ca	239	96	204
Fe	0.04	<0.10	3.03
K	16.8	28.5	5.9
Li (µg/l)	290	1684	55
Mg	12.0	4.4	98.5
Mn	0.71	0.14	0.561
Na	81	216	48.3
SiO_2	256	374	157
Sr	3.25	2.74	1.49
DIC	86	38	513
SO_4^{2-}	669	627	294
Cl^-	4.4	46.7	7.6

All units in mg/l unless noted otherwise. DIC as HCO_3^- equivalent.
Original data reported in Smith et al. (2010).

Table 2: Water chemistry data for Rembokola stream samples.

Sample	**a**	**b**	**c**	**d**	**e**	**f**	**g**	**h**	**i**	**j**	**k**
Distance (km)	0.00	0.01	0.11	0.30	0.61	0.86	1.13	1.48	1.73	1.98	2.21
T (°C)	72	75	52	45	40	38	35	35	34	33	31
pH	7.9	8.1	8.5	8.7	8.8	8.6	8.5	8.6	8.6	8.5	8.5
DIC	72	62	49	44	42	47	53	47	44	47	49
Al (µg/l)	7	6	3	bdl	2	3	bdl	2	2	4	9
As (µg/l)	68	65	66	69	70	70	73	69	72	73	69
Ca	169	152	152	153	152	153	155	154	154	153	154
Fe	0.04	0.03	0.03	0.03	bdl	bdl	bdl	bdl	bdl	0.03	0.03
K	25.6	26.2	28.1	28.5	28.3	28.5	29	29	28.7	28.5	28.3
Mg	8.8	7.7	8	8	8	8.1	8.3	8.2	8.2	8.2	8.2
Mn	0.39	0.33	0.31	0.22	0.15	0.15	0.14	0.08	0.07	0.07	0.08
Na	174.8	184.1	198.1	200.6	200.4	203.3	202.7	203.9	203.6	202.4	200.9
Si	160	164	172	165	154	150	148	142	141	136	135
SO_4^{2-}	684	668	696	710	711	719	715	716	717	713	713
Cl^-	38	38.9	43	42.9	42.8	44	43.4	44	43.8	43	43.9
CBE (%)	5	5	4	3	4	4	3	4	4	4	5

All values in mg/l unless noted otherwise. bdl = below detection limits; DIC = dissolved inorganic carbon as mg/l HCO_3^- eqv.; CBE = charge balance error. Full trace element analyses available in Supplementary Data.

Table 3: Water chemistry data for Tanginakulu stream samples.

Sample	l	m	n	o
Distance (km)	0.00	0.24	0.56	1.00
T (°C)	35.4	32	29.9	28
pH	8.1	8.1	8.4	8.5
DIC	295	232	199	163
Al (µg/l)	13	bdl	3	bdl
As (µg/l)	7	8	10	11
Ca	166	113	88	82
Fe	0.06	0.02	bdl	bdl
K	5.8	5.7	6.0	5.2
Mg	76.9	75.2	79.5	54.1
Mn	0.18	0.01	bdl	bdl
Na	40.9	40.0	43.0	33.7
Si	60	60	62	53
SO_4^{2-}	286	268	266	190
Cl^-	7.5	6.8	7.6	8.0
CBE (%)	24	17	19	19

All values in mg/l unless noted otherwise. bdl = below detection limits; DIC = dissolved inorganic carbon as mg/l HCO_3^- eqv.; CBE = charge balance error. High CBE may be a result of carbonate speciation (i.e. CO_3^{2-}> HCO_3^-), or unanalysed HS^-. Full trace element analyses available in Supplementary Data.

Stream	Map Ref.	Sample Type	Preparation	Sample Number	Al mg/kg	As mg/kg	Ca wt %	Cu mg/kg	Fe mg/kg	K mg/kg	Li mg/kg	Mg mg/kg	Mn mg/kg	Na mg/kg	Rb mg/kg	S wt%	Sr mg/kg	Ti mg/kg	V mg/kg
				Detection Limits:	**196**	**0.2**	**0.08**	**0.5**	**23**	**28**	**0.4**	**74**	**8**	**286**	**0.08**	**0.31**	**14**	**4**	**0.1**
Rem.	a	Terraced sinter	Bulk	497	–	1.7	0.2	–	44	195	6.6	174	67	619	1.89	–	47	–	0.5
Rem.	b	Spiculose sinter	Bulk	486	3511	40.9	6.2	2.3	1413	1363	18.7	11526	1118	3455	7.69	2.24	1373	70	2.9
Rem.	c	Layered sinter	Opal-A Layer	484 a	9051	5.1	1.8	7.4	4570	1285	3.9	2478	3338	4119	3.30	–	278	171	11.3
Rem.	c	Layered sinter	Opal-A Layer	484 b	6982	4.7	1.6	7.5	3330	1083	3.5	1779	2573	3310	2.79	–	264	133	8.3
Rem.	d	Layered MSC	Carbonate Layer	482 a	326	357	42.1	5.8	2162	278	7.0	2005	9488	748	0.61	1.71	4598	12	0.6
Rem.	d	Layered MSC	Opal-A Layer	482 b	1219	17.8	2.0	10.0	2579	360	2.3	3137	2148	526	1.81	–	246	64	3.7
Rem.	d	Layered MSC	Opal-A Layer	482 c	2457	18.1	3.9	15.6	3504	626	3.2	4076	3471	807	1.86	–	588	94	7.0
Rem.	d	Layered MSC	Carbonate Layer	482 d	523	254	34.5	7.2	1225	245	10.5	2009	6172	617	0.51	1.06	3210	19	0.7
Rem.	d	Layered MSC	Carbonate Layer	482 e	2719	378	37.4	20.1	4442	681	31.6	2779	6273	1786	1.78	1.00	3227	152	8.4
Rem.	g	Layered sinter	Opal-A Layer	475 a	1413	1.8	1.0	3.9	928	336	2.8	1928	2552	671	1.37	–	156	47	2.8
Rem.	g	Layered sinter	Opal-A Layer	475 b	7226	1.9	1.1	9.1	4865	1262	3.8	2303	3118	3299	3.80	–	220	181	14.7
Tan.	l	Travertine	Carbonate Layer	425 a	–	15.3	42.6	1.2	9293	42	0.6	722	384	506	0.14	–	3280	8	0.5
Tan.	l	Travertine	Carbonate Layer	425 b	–	80.4	35.5	2.6	40402	123	0.5	1426	582	393	0.55	–	3060	–	0.3
Tan.	l	Travertine	Carbonate Layer	425 c	–	7.7	19.8	–	2383	59	–	631	346	342	–	–	2849	–	–
Tan.	m	Travertine	Carbonate Layer	434 a	–	8.9	17.7	2.4	1554	65	1.6	6070	451	–	0.20	–	1307	8	0.5
Tan.	m	Travertine	Carbonate Layer	434 b	–	10.4	19.5	3.2	2498	93	1.0	6063	754	–	0.17	–	676	9	0.8
Tan.	m	Travertine	Carbonate Layer	434 c	–	12.1	25.0	2.4	3436	141	1.5	8253	550	395	0.26	–	1223	78	1.0
Pog.		Lobate MSC	Bulk	501	3184	0.4	23.9	0.6	1079	1294	1.7	123	938	893	1.56	0.62	3677	247	2.4
Pog.		Lobate MSC	Bulk	502	32890	0.7	21.7	7.7	2024	6002	10.4	158	312	15584	9.23	0.63	3975	492	14.3
Pog.		Layered MSC	Carbonate Layer	505 a	–	–	26.4	–	332	254	3.5	82	758	543	0.36	0.33	5764	43	0.3
Pog.		Layered MSC	Carbonate Layer	505 b	–	–	41.2	130	603	93	1.1	1429	14021	380	0.23	1.29	2587	11	–
Pog.		Layered MSC	Carbonate Layer	505 c	–	–	30.8	0.6	171	–	0.8	81	893	314	–	–	5080	–	–
Pog.		Spiculose sinter	Bulk	506	431	–	17.4	2.2	1067	307	3.0	8392	1853	688	1.18	3.48	2326	6	0.4

Rem. = Rembokola; Tan. = Tanginakulu; Pog. = Poghorovorughala. MSC = Mixed silica carbonate. Dash in cell indicates analyte below detection limits.

Table 4: Whole rock sinter and travertine chemistry.

Stream	Map	Sample	Sample	Ag	As	Au	Bi	Cd	Cu	Hg	Mo	Pb	Sb	Se	Te	Zn

	Ref.	Type	Number	µg/kg	mg/kg	µg/kg	mg/kg	mg/kg	mg/kg	µg/kg	mg/kg	mg/kg	mg/kg	mg/kg	µg/kg	mg/kg
			Detection Limits:	2	0.1	0.2	0.02	0.01	0.01	5	0.01	0.01	0.02	0.1	20	0.1
Rem.	d	Layered MSC	SV482	3	303	1.9	–	0.11	4.19	14	0.11	0.13	0.03	0.2	300	3.6
Rem.	e	Layered sinter	SV479	9	3.1	1.3	0.02	0.02	18.23	25	0.84	0.72	0.03	0.2	40	18.2
Rem.	g	Layered sinter	SV475	6	2.1	2.9	–	0.04	10.18	17	0.28	0.34	0.02	0.4	40	6.9
Tan.	l	Travertine	SV425	–	54	–	–	0.05	0.37	–	0.04	0.03	0.09	0.2	410	21.0
Pog.		Layered MSC	SV505	3	0.7	–	–	–	0.67	9	0.09	1.25	–	–	250	5.6
Pog.		Layered MSC	SV514	–	0.6	–	–	–	0.15	–	0.08	0.08	–	0.1	380	0.3

Rem. = Rembokola; Tan. = Tanginakulu; Pog. = Poghorovorughala. MSC = Mixed silica carbonate. Dash in cell indicates analyte below detection limits.

Table 5: Whole rock sinter and travertine chemistry – elements of significance to mineral exploration